

Optimized Monitor Placement for Accurate QoT Assessment in Core Optical Networks

Marianna Angelou, Yvan Pointurier, Davide Careglio, Salvatore Spadaro, and Ioannis Tomkos

Abstract—Network operators deploy optical monitors to ensure uninterrupted network operation and high quality of service. To achieve this they seek efficient design solutions that also maximize the benefit of their investments. In this work we present a monitoring technique that utilizes *partial* physical layer information generated by only a small set of monitors deployed in a mesh optical network to assess the quality of transmission (QoT) of all the established connections. The proposed method focuses on the *placement* of the monitors and on the minimization of the required monitoring equipment. We develop a heuristic that takes advantage of the attribute of certain end-to-end impairments that accumulate *additively* along the established lightpaths in order to find the optimum locations of a reduced number of available monitors. When monitoring a subset of the established lightpaths, it is possible to estimate the monitored QoT-related metric for all lightpaths leveraging the correlation between the connections sharing common links. The proposed algorithm efficiently selects the monitor locations that maximize the estimation accuracy. Extensive simulation studies show that the heuristic provides solutions close to the optimum and demonstrate that only a fraction of all the available monitor locations (1/4 or 1/3) need to be equipped, leading to significant cost savings. The monitor placement solutions are evaluated for core optical networks of different scales in the presence of static and incremental traffic.

Index Terms—Fiber optics communications; Monitoring; Networks; Optical network design.

I. INTRODUCTION

In view of the rapid growth of Internet traffic, optical performance monitoring (OPM) is essential in effectively managing high-capacity, wavelength-routed optical mesh networks [1]. In such networks, degradations, which can be static or dynamic, are induced by physical layer effects and accumulate along the lightpaths (a lightpath is the combination of a route and a wavelength) that transport the data and potentially affect the performance of the network's physical layer performance, measured for instance through the quality of transmission (QoT) of the carried signals. It is therefore

important for operators to use OPM in order to monitor their network at the physical layer and ensure that the network behaves as planned. In the past, techniques were proposed to monitor optical networks using partial information only, thereby decreasing the number of physical devices required to monitor the network [2]; however, the problem of placing these devices was not addressed. In this paper, we propose a monitor placement technique where monitor locations are chosen in order to maximize the accuracy of the monitoring scheme in the absence of full monitoring information in the network.

The applications of the estimation of signals' QoT based on (preferably) real-time measurements include lightpath provisioning, impairment mitigation, failure localization and maintenance. The continuous supervision of a network that can be dynamically reconfigured enables the concept of impairment-aware routing and wavelength assignment (RWA) where online connection demands can be routed based on educated QoT-constrained decisions [3]. In addition, optical monitors allow network operators to utilize the real-time feedback for dynamic mitigation of the impairments in order to meet the service level agreements established with their customers. Monitoring information can be further utilized for precise failure isolation that leads to fast and successful rerouting of the affected traffic [4] but also for fast troubleshooting of the physical failures. In this work, the topic of OPM is considered as the mechanism to assess the quality of the optical signal for any relevant application, such as those described above.

Monitoring is hence an important field in optical networking; for this reason various monitoring techniques, driven by the establishment of high-capacity optical transport that can be dynamically reconfigured, have been proposed during the past decade [5–8]. In the following, we assimilate *performance* monitoring (where several physical layer impairments are combined in a single metric such as the bit error ratio (BER)) to the terminology of *impairment* monitoring, where dedicated hardware equipment employs advanced monitoring techniques to measure individual physical layer impairments or performance metrics such as residual chromatic dispersion (CD) [9–11], polarization mode dispersion (PMD) [12,13], or the optical signal-to-noise ratio (OSNR) [14–16]. The proposed algorithms apply to both performance and impairment monitoring.

A monitoring scheme generally consists of two phases. In a first phase, during network planning, locations where monitoring devices are to be placed are chosen, using a *monitor placement algorithm*. This is the topic of this paper. Then, in a second phase, during network operation, the data from those monitors is collected in order to assess the performance of the network through some estimation framework. This second

Manuscript received June 9, 2011; revised November 4, 2011; accepted November 16, 2011; published December 7, 2011 (Doc. ID 148976).

Marianna Angelou (e-mail: marianna@ac.upc.edu) is with the Universitat Politècnica de Catalunya, C/ Jordi Girona 1-3, 08034 Barcelona, Spain, and is also with Athens Information Technology, 19.5km Markopoulou Avenue, 19002 Peania, Athens, Greece.

Yvan Pointurier is with Alcatel-Lucent Bell Labs, 91620 Nozay, France.

Davide Careglio and Salvatore Spadaro are with the Universitat Politècnica de Catalunya, C/ Jordi Girona 1-3, 08034 Barcelona, Spain.

Ioannis Tomkos is with Athens Information Technology, 19.5km Markopoulou Avenue, 19002 Peania, Athens, Greece.

Digital Object Identifier 10.1364/JOCN.4.000015

phase is out of the scope of this paper, which assumes that such an estimation framework is given. Specifically, we use the “network kriging” framework to perform the monitoring step itself [2,17]. The network kriging framework enables the estimation of the end-to-end metrics for all established lightpaths, given that only a subset of those are monitored, under some assumptions which are discussed further in this paper.

Placing an impairment monitor at the end of an optical lightpath feeds the network management system with an end-to-end real-time measurement of the monitored impairment. However placing a physical monitoring device at the receiver end of every link in the network is costly. Although network operators have to deploy optical monitors to ensure uninterrupted network operation, they also seek cost-effective deployment strategies that can maximize the benefit of their investment. As mentioned above, many works have dealt with impairment and performance monitoring; however, few studied the optimal *placement* of the monitoring equipment in view of QoT monitoring. In fact, all monitor placement techniques focused on a single application: failure localization [18–22], where the smallest set (preferably reduced to a single network element) of possible locations of a failure needs to be determined using the minimum amount of monitoring equipment. Our paper presents a placement algorithm that is more generic; it applies to QoT metrics which are continuous, while protection-oriented placement algorithms that target minimization problems are restricted to cases where metrics are integers or binary (a component has either failed or not failed). One notable exception is [17], where a placement algorithm is proposed in the context of IP network monitoring. That algorithm is compared with our proposed algorithm further in this paper. The placement technique proposed in this paper, referred to as pseudo-monitoring (PM), exploits the feedback received by only a small set of monitors that allows us, nonetheless, to estimate accurately the corresponding end-to-end metric of the lightpaths that are not monitored.

In this paper the performance of the placement algorithm is evaluated for network topologies of various scales and is compared to other placement methods. In addition, extensive simulations were performed to investigate the proximity of the PM solutions to the optimum. The algorithm was tested under static and incremental traffic conditions. The paper is organized as follows: The network model, notations, and problem statement are given in Section II. The proposed PM placement algorithm, along with a simpler heuristic and the QR placement algorithm from [17] are described in Section III. Section IV discusses the optimization capability of the proposed algorithm and presents the results from the application of all the considered placement methods in core networks of small (e.g., nation-wide) and large (e.g., pan-European) scale; it focuses on the static case where demand traffic is given. Section V tackles the dynamic case, where the network traffic increases. Finally Section VI concludes this paper.

II. MODELING AND PROBLEM FORMULATION

A. Notations

When planning a network it is critical to allocate the available resources in a cost-effective manner. Therefore in

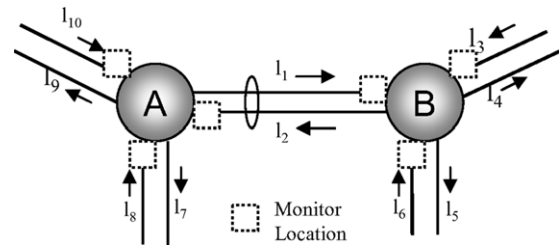


Fig. 1. Two nodes each with nodal degree of 3 are connected with a pair of unidirectional links. Monitors may be placed at the drop points of the nodes, yielding six possible monitor locations.

the context of monitor deployment, the goal is to be able to monitor the entire network with a limited number of devices. As shown in [2], there exists a trade-off between the number of deployed monitors and the overall monitoring accuracy achieved in the network. However, in [2] the problem of optimal monitor placement, that is, selecting the locations for a given number of monitors such that the network monitoring accuracy is maximized, was not tackled. This is the problem we tackle in this paper, and we introduce the formalism to solve it in this section.

The monitor placement technique that we propose here applies to mesh WDM networks without wavelength conversion; however, adaptation of the technique to networks with wavelength converters is straightforward as will be seen in Subsection IV.C. Consider a network graph $G(V, E)$ with a set of nodes V (e.g., optical crossconnects or OXC) and a set of unidirectional links E . To measure the end-to-end performance metric or impairment (e.g., OSNR, CD, or PMD) of a lightpath, a dedicated monitoring device has to be placed at the receiver end of that lightpath. It is assumed here that a monitor can only be placed at the drop ports of a node or, in other words, at the termination point (drop port) of a link, as shown in Fig. 1. Each of these monitors collects measurements for all the channels that are dropped at this link. Consequently there are $|E|$ potential monitor locations; every node can be equipped with at most a number of monitoring devices equal to the node degree.

Assume that L lightpaths are established in the network. We denote by $R \in \{0, 1\}^{L \times |E|}$ the routing matrix corresponding to those lightpaths, where $R(i, j) = 1$ if lightpath i uses link j and $R(i, j) = 0$ otherwise. Denote by $y \in \mathbb{R}^L$ an end-to-end metric related to the QoT of a lightpath, that accumulates linearly along a lightpath. Examples of metrics that behave in this fashion are given in Subsection II.D. Column-vector y contains the end-to-end metric for each established lightpath. Some of those lightpaths are monitored, and the others are not monitored. Without loss of generality, we reorder the rows of R and the elements of y such that $R = [R_{mon}^T, R_{nmon}^T]^T$ and $y = [y_{mon}^T, y_{nmon}^T]^T$, where R_{mon} and R_{nmon} describe the lightpaths that are monitored and not monitored, respectively, and y_{mon} and y_{nmon} contain the metrics for the lightpaths that are monitored and not monitored, respectively.

B. Estimation Framework

Having partial information about a link-additive impairment from monitors located throughout a network, it is

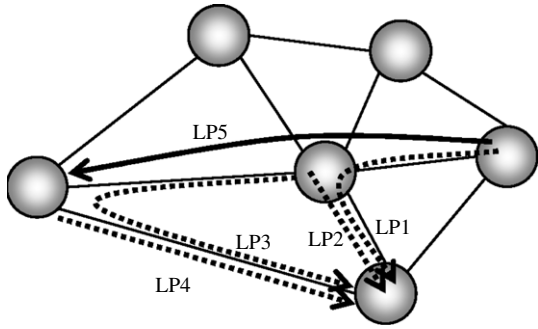


Fig. 2. It is possible to use monitoring measurements collected from a subset of all the network lightpaths (LP1, LP2, LP3, LP4) to estimate accurately the corresponding end-to-end metric (e.g., OSNR) of a lightpath that is not monitored (LP5) using the “network kriging” estimation framework [2,17,23]. Placing monitoring devices at the termination points of LP1, LP2, LP3, and LP4 would allow the operator to also estimate the QoT of LP5 using only partial network information.

possible to use a linear estimator to derive the impact of the impairment even for the lightpaths that are not monitored (Fig. 2). This work utilizes the so-called “network kriging” (NK) [17] estimation framework that essentially leverages the correlation between lightpaths that share links. In the NK framework the network traffic is abstracted through the routing matrix R . The accuracy of the estimates is assessed through the ℓ_2 norm: the network kriging estimator is the linear estimator that maximizes monitoring accuracy, i.e., it returns the vector \hat{y}_{nmon} with minimum ℓ_2 norm, given the routing matrix $R = [R_{nmon}^T, R_{mon}^T]^T$ and the monitored data y_{mon} . The closed form for this estimate is [17]

$$\hat{y}_{nmon} = R_{nmon} R_{mon} (R_{nmon} R_{mon}^T)^+ y_{mon}, \quad (1)$$

where $(\cdot)^+$ denotes a matrix pseudo-inverse such as the Moore–Penrose inverse.

C. Problem Formulation

Assume that we are given only $m \leq |E|$ monitors to install in a network, where lightpaths are routed according to R . Then it is not possible to monitor every lightpath in the network and the QoT of any non-monitored lightpath must be estimated with the estimation framework described in Subsection II.B. Let \mathcal{E}_m be the set of all subsets of E of size m ($\forall F \in \mathcal{E}_m: F \subset E$ and $|F| = m$). \mathcal{E}_m represents the set of all possible monitor placements (placement of m monitors). Each monitor placement (a set of m locations) determines exactly $R_{mon}, R_{nmon}, y_{mon}$, and y_{nmon} , and hence \hat{y}_{nmon} . In other words, the mapping f such that $\hat{y}_{nmon} = f(F)$, where $F \in \mathcal{E}_m$, is well defined. We define the network monitoring accuracy as the ℓ_2 norm of the difference between the actual values of the QoT metrics of interest and the estimated QoT metrics, normalized by the ℓ_2 norm of the actual values of the QoT metrics of interest. Hence, if we monitor some metric with actual values y given a routing matrix R , monitor placement M , and unmonitored locations P , and if we let $\hat{y} = [y_{mon}^T, \hat{y}_{nmon}^T]^T$ (note that y_{mon} and \hat{y}_{nmon} are functions of R, M , and P), then

the accuracy of the monitoring scheme is

$$\text{rRMSE}(R, M, P) = \frac{\|y - \hat{y}\|}{\|y\|},$$

where $\|\cdot\|$ denotes the ℓ_2 norm. Note that the accuracy $\text{rRMSE}(R, M, P)$ is effectively the relative root mean square error of the QoT metric of interest. Hence the problem of monitor placement is to find the optimal placement $F^* \in \mathcal{E}_m$ such that

$$F^* = \underset{\mathcal{E}_m}{\text{argmin}} \frac{\|y - \hat{y}\|}{\|y\|}. \quad (2)$$

An exhaustive search to find F^* is very computationally expensive since $|\mathcal{E}_m| = \binom{|E|}{m}$, and heuristics are needed to solve Eq. (2). Before presenting heuristic algorithms that solve Eq. (2), we give more details on the physical layer model.

D. Modeling of the Physical Layer

In this study a mesh network topology is considered to be traversed by a number of preplanned transparent lightpaths. Cascades of erbium-doped fiber amplifiers between spans of transmission and dispersion-compensating fiber segments form typical WDM links. The physical layer impairments that are considered here are link additive over a path, meaning that the end-to-end parameter that corresponds to the entire lightpath can be computed by adding the link-level parameters of the impairment in question. In addition, it is assumed that there are hardware devices that can effectively measure each of these impairments; the optimized placement of these devices is the goal of this work. Examples of parameters that measure those impairments are i) OSNR, ii) PMD, iii) residual CD, and iv) nonlinear phase [24]. Using a combination of those four impairments, it is possible to compute the signal’s BER in intensity-modulated (non-coherent) systems [25]. More details on the link-additivity property of those parameters can be found in [23].

For the remainder of the paper a generic impairment that accumulates additively is considered, yet in the scenarios simulated in Sections IV and V we have assumed OSNR monitoring as the targeted application.

III. MONITOR PLACEMENT ALGORITHMS

We now describe three heuristics that solve problem (2). The first algorithm (our contribution) is called “pseudo-monitoring” (PM) and greedily removes monitors (starting from a situation where each link is equipped with a monitor) to iteratively minimize the estimation error for the lightpaths that are not equipped with monitors. The second algorithm (also our contribution), called “busy link” (BL), is a simplification of the first heuristic, which is used to demonstrate that the complications of the PM algorithm are indeed needed to achieve good performance. The third algorithm, called QR, was proposed in [17].

Input: graph G , links E , lightpaths R , desired number of monitors m , accuracy threshold ϵ

Output: $M \subset E$: hardware monitor locations, $PM \subset E$: pseudo-monitor locations.

- 1) Using E and R : let B be the sorted list of links in ascending busyness.
- 2) $M = B$; $PM = \{\}$; $c=0$;
- 3) **for** $j \in B$ (from least to most busy link)
- 4) $M' = M \setminus \{j\}$; $PM' = B \cup \{M'\}$;
- 5) $c = \text{rRMSE}(R, M', PM')$;
- 6) **if** $c \leq \epsilon$; $M = M'$; $PM = PM'$; **end if**
- 7) **if** $|M| = m$; **return**; **end if**
- 8) **end for**
- 9) **for** $j \in M$
- 10) $\text{cost}(j) = \text{rRMSE}(R, M \setminus \{j\}, B \cup \{M'\})$;
- 11) **end for**
- 12) Rank $\text{cost}(\cdot)$ in descending order to place monitors on the $|M| - m$ locations with lowest cost .

Fig. 3. Pseudo-monitoring monitor placement algorithm.

A. The Pseudo-Monitoring Heuristic

The algorithm (Fig. 3) is a greedy heuristic that starts by assuming that all monitoring locations are equipped and sequentially removes the monitors that contribute the least with their measurements to the estimation process (NK). The algorithm relies on the notion of a “busy link”: the “busyness” of a link is the number of connections that are terminated at this link. The busier a link, the more connections can be monitored by this link, and hence the more information a monitor located at this link can gather about the network. Note that it is not only the amount of information about the network that we can collect which matters, but also how the information collected by several monitors can be correlated. Hence, it is not always a good strategy to select the busiest links as monitor locations, as will be shown in Section IV. Given this, our proposed PM algorithm consists of three phases.

In the first phase (Fig. 3, line 1), or “preprocessing phase,” the links are sorted by ascending busyness. All links are fitted with monitors (line 2).

Then, in the second phase (lines 3–8), the list of links is scanned (line 3) and, for each link in the list, we tentatively remove the monitor installed at this link (line 4): an end-to-end metric for any lightpath terminated at this link would need to be estimated rather than monitored. We evaluate the impact of removing the monitor from this location on the monitoring accuracy as follows. We define the overall network monitoring accuracy metric $\text{rRMSE}(R, M, P)$ as in Subsection II.C for the network defined by the routing matrix R , monitor locations M , and unmonitored locations P .

At network planning time, physical measurements of a number of metrics such as the OSNR are not available, as real deployment of monitors would be required to obtain that data. Instead, realizing that the NK estimator can be used on any link-additive metric, we use lightpaths and link physical lengths (the total length of a lightpath is the sum of the lengths of the links of this lightpath) to compute the $\text{rRMSE}(R, M, P)$ figure of merit. If this metric is smaller than a predefined accuracy threshold ϵ , then it is possible to replace the physical

monitor with an estimate, and the selected location is removed for good from the list (line 6). The process repeats until only m monitors are left, or when there is no more link to assess (line 7).

It is possible that, after examining all links, the algorithm has not been able to remove enough locations from the list and that $|M| > m$ locations are retained. In this case, the third phase starts in order to remove the extra $|M| - m$ monitors. In this phase (lines 9–12), for each remaining possible link/monitor location, the rRMSE metric is evaluated assuming that the considered link is not fitted with a monitor (lines 9–11). This list of rRMSE is ordered in descending order and links corresponding to the $|M| - m$ highest rRMSE metrics are selected as additional monitor locations (line 12).

Note that any link-additive metric can be used in the planning phase to determine monitor placement, since the network kriging estimator relies on the link-additivity property. The performance of the estimator during the operation phase depends on the monitor placement and hence on the metric used during planning. Link length is a suitable metric because many impairments grow (although not necessarily proportionally) with transmission distance, and hence link length gives a good indication of the intensity of the impairments sustained by a signal propagated within a link. It is possible to use other metrics than link length in the planning phase; however, the problem of choosing and comparing the choices for such a metric is outside the scope of this paper; in addition, we will observe in Section IV that the chosen metric yields relatively small estimation errors, such that the quest for another metric to be used in the planning phase may not yield substantial benefits.

B. The Busy Link Heuristic

The busy link heuristic is a much simplified version of the PM heuristic, which essentially consists solely of the first phase of PM. Links are sorted by ascending busyness, and the m busiest links are fitted with monitors. As indicated above the rationale for this is that busiest links tend to collect more information about the network.

C. The QR Heuristic

The monitor placement problem was also tackled by the authors in [17] using an algebraic method based on QR decompositions of routing matrices (further referred to as the QR method). In [17] the authors argue that the selection of routes within R to minimize estimation errors amounts to the so-called “subset selection” problem (finding the set of the rows of G such that the space spanned by those rows matches as closely as possible the space spanned by all rows of R), which is NP-complete. A good heuristic to solve this problem consists of using a QR factorization of R with column pivoting to select the first m left singular vectors of R . The reader is referred to [17, Section III-B] for further details about this heuristic.

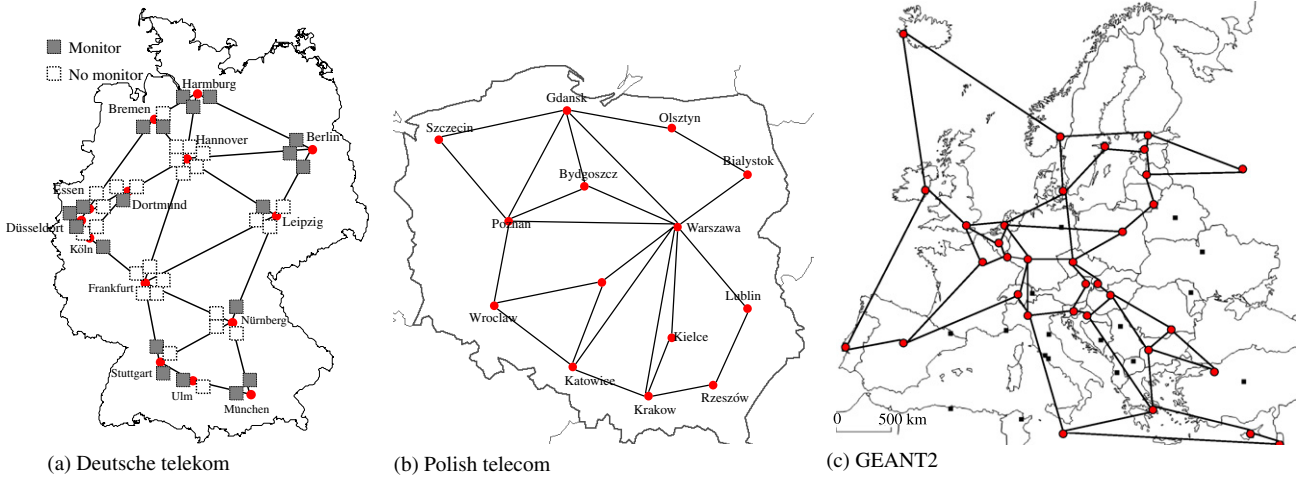


Fig. 4. (Color online) The three topologies considered in this paper: two country-sized networks (Deutsche Telekom and Polish Telekom) and a continent-sized network (GEANT2). The Deutsche Telekom backbone network is shown with 20 monitored locations resulting from the PM placement.

TABLE I
NETWORK TOPOLOGIES SPECIFICATIONS

Topology Name	Deutsche Telekom (DT)	Polish Telekom (TP)	GEANT2
No. of unidirectional links	46	48	104
No. of nodes	14	14	34
Node degree	3.29 (min. 2, max. 6)	3.42 (min. 2, max. 9)	3.18 (min. 2, max. 5)

IV. NUMERICAL RESULTS

A. Performance Evaluation

To test the monitor placement methods, the algorithms are applied to three different meshed topologies (Fig. 4 and Table I) using traffic matrices of varying load. A traffic load of 1 corresponds to the establishment of $|V|(|V|-1)$ lightpaths in a topology with V nodes. The placement algorithms are evaluated using the OSNR as the monitored metric. Note that the OSNR is indeed link-additive through its inverse since $OSNR_{tot} = \left(\sum \frac{1}{OSNR_i}\right)^{-1}$, where $OSNR_{tot}$ is the OSNR for a lightpath and $OSNR_i$ is the OSNR for the i th hop of that lightpath; hence the estimation and placement frameworks described above apply to OSNR monitoring. To evaluate the OSNR, we consider the chain of optical amplifiers that the signal traverses along a lightpath and compute the end-to-end OSNR due to the amplified spontaneous emission (ASE) noise [26]. The amplifier spans are assumed to be 80 km long, and the noise figure of the amplifiers is set at 6 dB. The ϵ threshold used by the PM algorithm is set to 10^{-9} .

For a given load, every traffic matrix is served by an equivalent number of lightpaths computed by a k -shortest path RWA process assuming 80 wavelengths available per fiber in a single-rate WDM transmission system. For the Deutsche Telekom (DT) topology depicted in Fig. 4(a) that consists of 14 nodes and 46 unidirectional links, a traffic matrix of load

1 corresponds to 182 traffic demands. The demands are drawn randomly uniformly among all possible (source, destination) pairs of nodes.

Figure 4(a) illustrates the monitor placement solution returned by the PM algorithm for a certain set of lightpaths traversing the DT topology, where $m = 20$ links out of the possible 46 locations are equipped with monitors. Using a random traffic generator, 50 different traffic matrices all corresponding to load equal to 2 are fed as input to the PM, QR, and BL monitor placement algorithms for the same topology (DT). The three algorithms along with a random placement method are tested for a range of available monitors from 5 to 35 (Fig. 5). To compare their performance, the mean rRMSE of all 50 traffic matrices are reported, along with error bars corresponding to one standard deviation around the mean relative RMSE. Particularly for the random placement, each of the 50 traffic matrices 50 random solutions were generated (i.e., mean rRMSE from a total of 2500 solutions) for each case of available monitors. The lower the rRMSE the more powerful the placement solution. PM outperforms the other techniques for the entire range of available monitors as its solutions yield the highest estimation accuracy (lowest mean rRMSE). Indeed it is observed that 15 locations out of the total 46 are only required to be equipped if the target OSNR estimation accuracy is 1%.

Estimation as done by the kriging framework is facilitated when the energy of the unobserved lightpaths, when projected

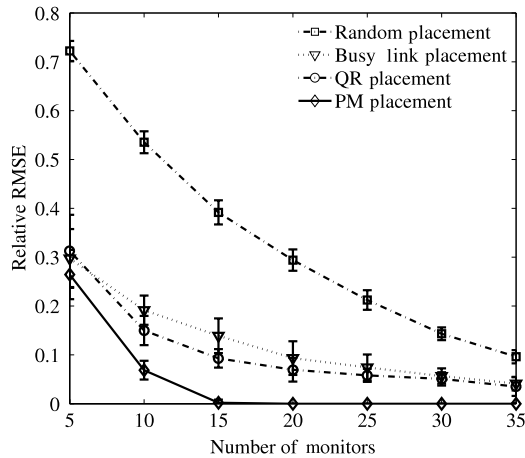


Fig. 5. Comparison of the placement techniques for the Deutsche Telekom (DT) network. The averaged relative root mean square error was computed for all placement methods applied in the DT backbone network for traffic load equal to 2, i.e., 2 connections on average per pair of nodes. With the PM heuristic, 15 monitors out of the possible 46 locations are enough to yield an estimation error for the OSNR below 1%.

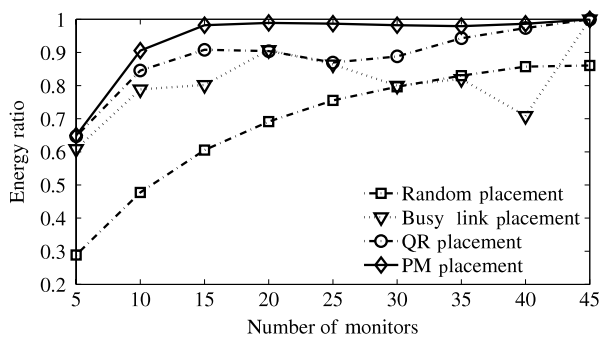


Fig. 6. Fraction of the energy (“energy ratio”) of the unobserved lightpaths that lies in the space spanned by the observed lightpaths for the DT topology with a load of 2. The energy ratio is higher when more information about the unobserved lightpaths is known through the observation of other lightpaths with the deployed monitors.

onto the subspace spanned by the observed lightpaths, is small [2]. Indeed such small energy means that the observed lightpaths capture most of the information regarding the unobserved lightpaths. In Fig. 6 we depict, for each placement algorithm and for the DT topology with a load of 2, the average fraction of the energy (“energy ratio”) of the unobserved lightpaths that lies in the space spanned by the observed lightpaths. This fraction increases with the number of monitors (and hence of observed lightpaths and of the captured information about the unobserved lightpaths) for the proposed PM placement algorithm. The energy ratio is significantly larger for PM than for the other considered algorithms. The energy ratio decrease that is observed for the busy link and the QR algorithms for 20 to 25 (QR) or 40 (busy link) monitors may seem counterintuitive but can be explained like this: although with a large number of monitors few lightpaths are unobserved, little is known about them through the observed lightpaths. This is to be contrasted with PM, which gradually

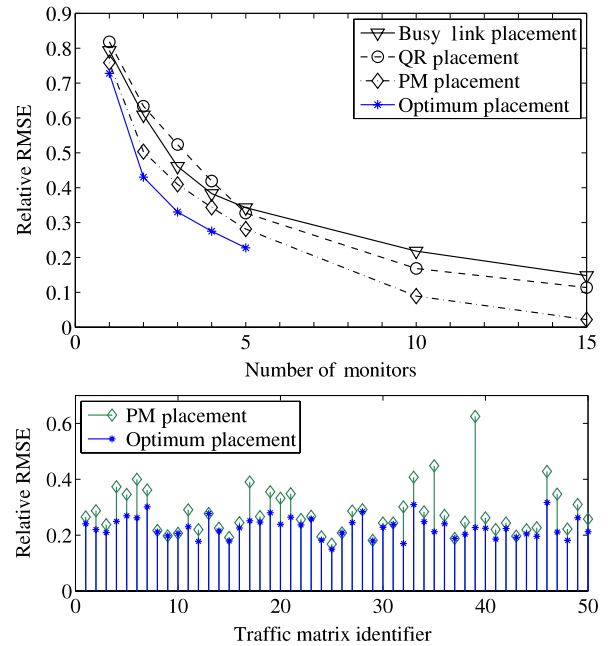


Fig. 7. (Color online) Comparison of optimum solutions against the solutions retrieved by the three heuristics for the DT topology; the resulting error is the average of 50 randomly generated traffic matrices of load equal to 1 (top). PM and optimum relative RMSE error results for each of the 50 traffic matrices when 5 monitored locations are assumed (bottom).

collects information about all lightpaths as more monitors are deployed.

B. Gap to Optimality

Having compared PM with the other methods, extensive simulations (i.e., an exhaustive search across the full solution space) are run to investigate how close PM is from the optimum placement solution. For a given topology the total number of possible placement solutions is calculated by $|\mathcal{E}_m| = \binom{|E|}{m}$, where E is the set of unidirectional links and m is the number of monitors to be deployed. Consider, for instance, the DT topology ($|E| = 46$) and $m = 5$ available monitors; the total possible solutions sum up to 1,370,754. The number becomes prohibitively large for $m > 5$. Hence this effort is inevitably constrained by the required processing time and is limited to the optimum solutions for $m = 1, 2, \dots, 5$. Obviously an operator would not install only 1 or even 5 monitors in their network as this would not allow accurate performance estimations; this range was merely selected to demonstrate the performance of PM compared with the optimum when possible.

All the possible placement solutions for $m = 1, 2, \dots, 5$ were enumerated and evaluated using the NK estimation framework for a set of 50 different traffic matrices of load equal to 1. The optimum solution, i.e., the one with the lowest relative error, was retrieved and compared to the corresponding solutions of PM, QR, and BL as depicted in Fig. 7 (top). Taking into account the sequential nature of the heuristic and noticing the rapid decrease of the relative error of the PM solutions with the increasing number of monitors in the

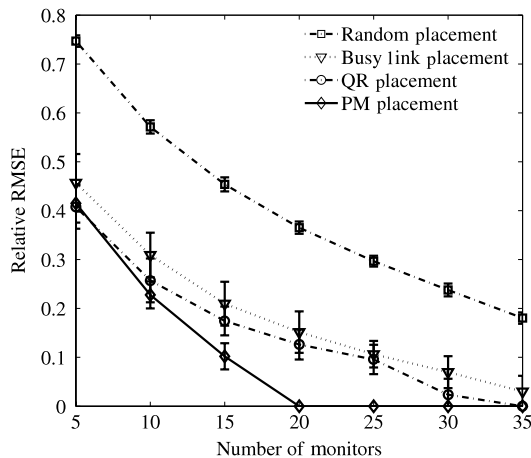


Fig. 8. Averaged relative RMSE of all placement methods applied on the Polish Telecom topology. The traffic load is equal to 2.

various network topologies, we observe that $m = 5$ monitors (over $|E| = 46$ locations in total) is a small number for PM to display its capabilities. Nonetheless based on the simulation results, the PM algorithm approaches the optimum solution within 5% (in terms of relative RMSE gap) for the case of 5 monitors.

Figure 7 (bottom) depicts the raw RMSE for both the optimum and the PM algorithm for every considered input traffic matrix for $m = 5$; except for a small number of traffic matrices, the gap between PM and the optimal solution is fairly uniform across all the tested traffic matrices.

C. Scalability of the Monitor Placement Methods With Network Size

The optimized monitor placement is subjected to another meshed topology of the same scale as DT, yet with different connectivity characteristics. The goal of this experiment is to investigate the locations the proposed monitor placement selects in a commercial topology that is not evenly meshed, i.e., a topology where nodal degree is highly spread. It is expected that a topology with nodes that are not well connected would require more monitored locations to achieve acceptable accuracy.

The selected topology is the Polish Telecom backbone network (further denoted as TP) that consists of 14 nodes and 48 unidirectional links. As depicted in Fig. 4(b), and unlike the DT topology, TP has one highly connected node (Warsaw, degree 9) and several nodes with degree 2. As with the DT topology, PM, QR, BL, and the random selection of locations are evaluated through the relative RMSE with respect to the variable number of monitors. The results are averaged over 50 different randomly generated traffic matrices of load equal to 2, corresponding to 364 lightpaths. As shown in Fig. 8, PM demonstrates a relatively high estimation error for a low number of monitors (errors higher than with the DT topology) that, nevertheless, improves fast with additional monitored locations. With $m = 20$ monitors out of a possible $|E| = 48$ locations the accuracy is better than 1% with PM, whereas it is still above 10% with the other techniques. The other

algorithms require more than 30 monitors to achieve the same level (1%) of accuracy.

Focusing on the PM and QR techniques, the experiments for the TP topology are extended for traffic scenarios with load from 1 up to 3 in order to investigate the dependence of the monitor placement techniques on the induced traffic load. As illustrated in Fig. 9, PM experiences the same sharp decrease of the relative error at every monitor addition step that converges to < 1% for $m \geq 20$ monitors regardless of the traffic load. What is more, the estimation accuracy of PM and QR (the two techniques that perform best in terms of accuracy) are not affected by the increasing traffic.

Having universal supervision of the network status with a limited amount of physical resources becomes particularly important when considering large-scale networks that may span a continent. Therefore, in addition to the standard nation-wide topologies, the optimization capability of the placement techniques is also tested in a topology of larger scale, i.e., GEANT2 (Fig. 4(c)). GEANT2 is by nature a translucent network, meaning that at least sparse regeneration of the optical signal may be required to ensure transmission with acceptable QoT. In this experiment no regeneration is assumed. The goal of this exercise is to focus on the scalability of the algorithms; besides the monitor placement techniques employed in this work do not depend on the physical lengths of the links. Note though that in the presence of regenerators the PM and QR algorithms could be adapted in the following simple fashion: consider a regenerator placed at an intermediate node of a lightpath. In the routing matrix R this lightpath is replaced by two lightpaths, one being the segment of the original lightpath from the source node to the regenerator location and the second from the regenerator to the termination point. In this way this lightpath contributes with physical information both from the regenerated and the non-regenerated parts.

In the GEANT2 topology, 34 nodes are interconnected with 104 unidirectional links. The same transmission and link design parameters as in the smaller topologies are used. Again 50 different traffic matrices are generated randomly for traffic loads of 0.5 and 1, corresponding to 561 and 1122 lightpaths, respectively. The solutions retrieved by the algorithms are evaluated through their estimation accuracy (relative RMSE). As depicted in Fig. 10, PM performs significantly better than the other techniques for both traffic scenarios, demonstrating the same sharp decrease in estimation error, reaching a relative error of less than 1% for as few as 25 monitors (for a load of 1) out of a total of 104 possible locations.

V. MONITOR PLACEMENT IN THE PRESENCE OF DYNAMIC TRAFFIC

We have described in depth the performance of the proposed monitor placement algorithm (PM) when a static set of lightpaths is established in the network. In a dynamic optical network, the varying traffic can potentially affect the estimation accuracy of the deployed monitors, since lightpath terminations may vary while the monitor locations are de facto fixed at network planning time for the hardware monitors. Consider a set of deployed monitors for a given

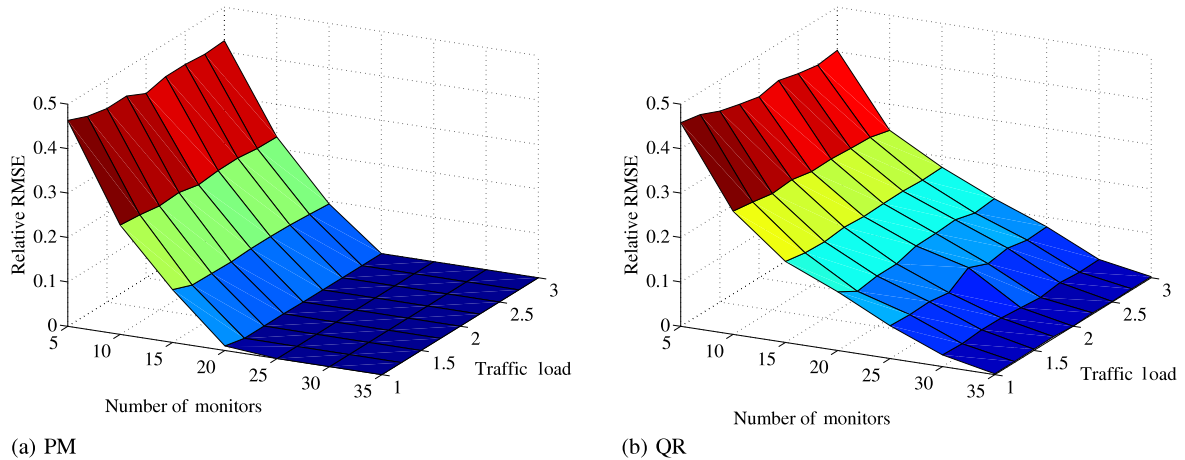


Fig. 9. (Color online) Relative RMSE for the PM and QR monitor placement methods with respect to the number of available monitors and increasing traffic load in the TP topology. PM and QR are not affected by the traffic load and PM achieves an estimation error below 1% for $m = 20$ deployed monitors.

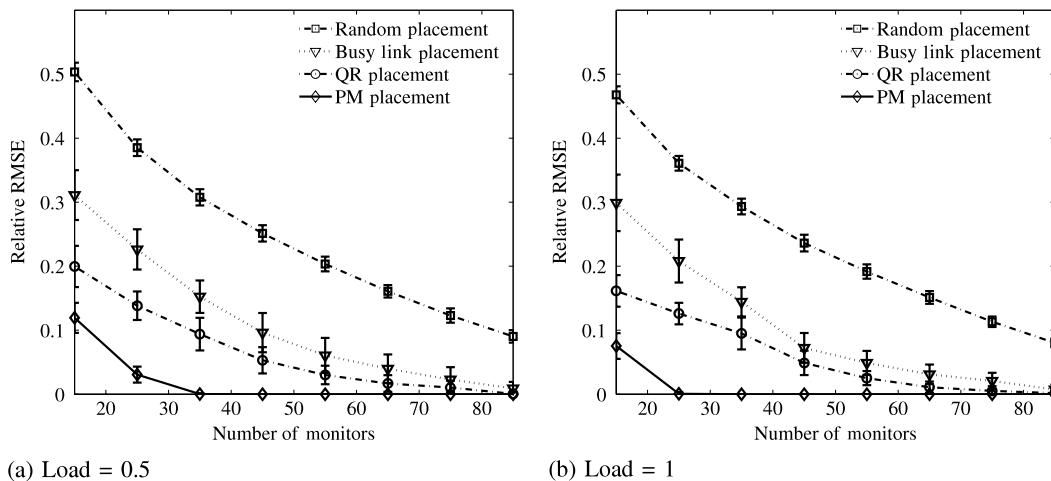


Fig. 10. Averaged relative root mean square error of all placement methods applied on the GEANT2 topology. PM achieves an estimation error below 1% for $m = 25$ monitored locations out of 104 available.

preplanned set of lightpaths. As traffic varies with time, new connections are getting established or existing ones are being torn down. Under such conditions the estimation accuracy of the monitoring technique may improve provided that more lightpaths terminate at monitored locations and that the monitored lightpaths provide the NK framework with enough information to estimate the unmonitored ones. The opposite effect would occur if the fraction of the traffic that is monitored becomes decorrelated with the unmonitored traffic.

In this context we examine several scenarios with incremental traffic. The investigation of a scenario with only incremental traffic was triggered by the constant and rapid increase of the IP traffic. We assume that a set of lightpaths corresponding to a traffic load equal to 1 are established in the DT backbone network. The PM algorithm is used to compute the locations for $m = 20$ monitors that are assumed fixed. We select 20 monitors as this is a sufficient number of monitors to accurately (error is below 1%, as mentioned in Subsection IV.A) supervise the global network traffic for load up to 3. To the

initial set of lightpaths (of total load 1) we add randomly generated “chunks” of traffic, each corresponding to a load of 0.25 (i.e., approximately 46 new lightpaths per chunk of added traffic). The additional traffic was set to 0.25 because a smaller set would not allow us to observe significant modifications in the estimation accuracy. Indeed we examined several similar scenarios (for different permutations of initial and additional traffic) and we observe that as more lightpaths are added, the estimation error increases, yet not beyond 5% as shown in Fig. 11 (dotted curve with square marks).

Furthermore, the PM algorithm was used to compute the optimized monitor locations in every increasing step, as if the monitors were *not* fixed. As depicted in Fig. 11 the solutions (plain curve, diamond marks) are compared to the predeployed one; it was observed by detailed comparison of the placement results that only 3 mutual replacements of monitors (i.e., removal of a monitor from a certain location and placement to another) would allow the estimation error to become approximately 0 again. In this example, when the

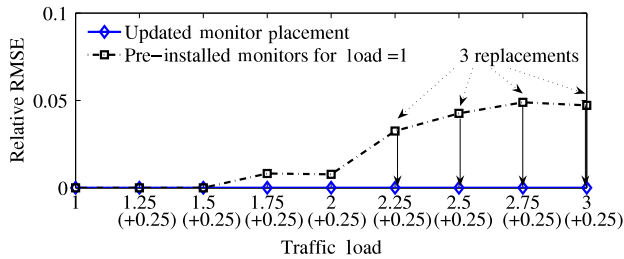


Fig. 11. (Color online) Example of monitor placement in the presence of varying incremental traffic. Twenty fixed equipped locations computed by the PM algorithm for a traffic matrix of load 1 are studied as “chunks” of traffic and are added to the already established lightpaths. Without installing additional monitors the estimation error becomes larger than 1% for a traffic load larger than 2. It was observed by inspection that only 3 (out of 20 possible) monitor displacements are sufficient to decrease the estimation error back to less than 1%.

traffic load becomes higher than 2, an operator may deem that the estimation accuracy is not acceptable. In such a case, moving (not adding) only 3 monitors to new locations is sufficient to accurately estimate again the QoT of all the traffic.

VI. CONCLUSION

This work leverages the correlation of the QoT of channels traversing a mesh topology and proposes a monitor placement framework that first decides the placement of the monitoring devices to a few strategically selected locations during the network planning phase and enables the universal supervision of all the established connections during network operation. The proposed heuristic (PM) outperformed other monitor placement methods in terms of monitoring accuracy or, equivalently, the number of monitors needed to achieve the same level of monitoring accuracy. It was indeed shown that through the efficient placement of monitors using the PM heuristic, only a fraction of the possible locations in a mesh topology need to be equipped—in the considered topologies only 1/4 or 1/3 of the possible monitor locations actually required a physical monitoring device in order to compute the QoT of all established lightpaths within a few percent; the unmonitored lightpaths have their QoT estimated, rather than directly measured. We also argued that the proposed technique scales well with the network size, as topologies ranging from less than 50 to more than 100 links were investigated for various static loads.

In addition, although the problem of monitoring placement is inherently a planning issue where monitors are physical devices that cannot be moved around easily during network operation, we also hinted that our placement technique is compatible with operation scenarios where the load of the network is incremental, i.e., lightpaths are added. In this case, the monitoring accuracy is little impaired by the changes in the network load, and, if an operator needs to maintain a very high monitoring accuracy even after a load increase, only a few monitors would need to be displaced, thereby reducing network operating expenditures compared with a situation where the monitoring scheme would change completely due to a change in the load.

ACKNOWLEDGMENTS

This paper is an extension to the work presented by the authors at OFC 2011 [27]. The authors would like to thank Dr. Siamak Azodolmolky for his valuable input during the course of this work. This work was partially supported by the European Commission through the FP7 CHRON project (258644).

REFERENCES

- [1] D. C. Kilper, R. Bach, D. J. Blumenthal, D. Einstein, T. Landolsi, L. Ostar, M. Preiss, and A. E. Willner, “Optical performance monitoring,” *J. Lightwave Technol.*, vol. 22, no. 1, pp. 294–304, Jan. 2004.
- [2] Y. Pointurier, M. Coates, and M. Rabbat, “Cross-layer monitoring in transparent optical networks,” *J. Opt. Commun. Netw.*, vol. 3, pp. 189–198, Mar. 2011.
- [3] S. Azodolmolky, M. Klinkowski, E. M. Tordera, D. Careglio, J. Solé-Pareta, and I. Tomkos, “A survey on physical layer impairments aware routing and wavelength assignment algorithms in optical networks,” *Comput. Netw.*, vol. 53, no. 7, pp. 926–944, May 2009.
- [4] C. Mas, I. Tomkos, and O. K. Tonguz, “Failure location algorithm for transparent optical networks,” *IEEE J. Sel. Areas Commun.*, vol. 23, no. 1, pp. 1508–1519, Jan. 2005.
- [5] M. Petersson, H. Sunnerud, M. Karlsson, and B.-E. Olsson, “Performance monitoring in optical networks using Stokes parameters,” *IEEE Photon. Technol. Lett.*, vol. 16, no. 2, pp. 686–688, Feb. 2004.
- [6] L. Mefflah, B. Thomsen, J. E. Mitchell, P. Bayvel, G. Lehmann, S. Santori, and B. Bollez, “Advanced optical performance monitoring for dynamically reconfigurable networks,” in *Proc. Networks and Optical Communication (NOC)*, 2005.
- [7] Y. K. Lizé, J.-Y. Yang, L. C. Christen, X. Wu, S. Nuccio, T. Wu, A. E. Willner, R. Kashyap, and F. Séguin, “Simultaneous and independent monitoring of OSNR, chromatic and polarization mode dispersion for NRZ-OOK, DPSK and duobinary,” in *Optical Fiber Communication Conf. and Expo. and the Nat. Fiber Optic Engineers Conf.*, 2007, OThN2.
- [8] S. L. Woodward, “Monitors to ensure the performance of photonic networks,” in *Optical Fiber Communication Conf. and Expo. and the Nat. Fiber Optic Engineers Conf.*, 2007, OMM1.
- [9] Y. Ku, C. Chan, and L. Chan, “Chromatic dispersion monitoring technique using birefringent fiber loop,” in *Optical Fiber Communication Conf. and Expo. and the Nat. Fiber Optic Engineers Conf.*, 2006, OFN2.
- [10] X. Yi, F. Buchali, W. Chen, and W. Shieh, “Chromatic dispersion monitoring in electronic dispersion equalizers using tapped delay lines,” *Opt. Express*, vol. 15, no. 2, pp. 312–315, Jan. 2007.
- [11] F. N. Khan, A. P. T. Lau, C. Lu, and P. K. A. Wai, “Chromatic dispersion monitoring for multiple modulation formats and data rates using sideband optical filtering and asynchronous amplitude sampling technique,” *Opt. Express*, vol. 19, no. 2, pp. 1007–1015, Jan. 2011.
- [12] G.-W. Lu, M.-H. Cheung, L.-K. Chen, and C.-K. Chan, “Simultaneous PMD and OSNR monitoring by enhanced RF spectral dip analysis assisted with a local large-DGD element,” *IEEE Photon. Technol. Lett.*, vol. 17, no. 12, pp. 2790–2792, Nov. 2005.
- [13] J. Yang, C. Yu, L. Cheng, Z. Li, C. Lu, A. P. T. Lau, H.-Y. Tam, and P. K. A. Wai, “CD-insensitive PMD monitoring based on RF power measurement,” *Opt. Express*, vol. 19, no. 2, pp. 1354–1359, Jan. 2011.
- [14] J. H. Lee, D. K. Jung, C. H. Kim, and Y. C. Chung, “OSNR monitoring technique using polarization-nulling method,” *IEEE Photon. Technol. Lett.*, vol. 13, no. 1, pp. 88–90, Jan. 2001.

- [15] L. Baker-Meflah, B. Thomsen, J. Mitchell, and P. Bayvel, "Simultaneous chromatic dispersion, polarization-mode-dispersion and OSNR monitoring at 40 Gbit/s," *Opt. Express*, vol. 19, no. 20, pp. 15999–16004, Sept. 2008.
- [16] J. Schröder, O. Brasier, T. D. Vo, M. A. F. Roelens, S. Frisken, and B. J. Eggleton, "Simultaneous multi-channel OSNR monitoring with a wavelength selective switch," *Opt. Express*, vol. 18, no. 21, pp. 22299–22304, Oct. 2010.
- [17] D. B. Chua, E. D. Kolaczyk, and M. Crovella, "Network kriging," *IEEE J. Sel. Areas Commun.*, vol. 24, no. 12, pp. 2263–2272, Dec. 2006.
- [18] S. Stanic, S. Subramaniam, H. Choi, G. Sahin, and H.-A. Choi, "On monitoring transparent optical networks," in *Proc. ICPPW*, 2002.
- [19] Y. G. Wen, V. Chan, and L. Z. Zheng, "Efficient fault diagnosis algorithms for all-optical WDM networks with probabilistic link failures," *J. Lightwave Technol.*, vol. 23, no. 10, pp. 3358–3371, Oct. 2005.
- [20] P. Nayek, S. Pal, B. Choudhury, A. Mukherjee, D. Saha, and M. Nasipuri, "Optimal monitor placement scheme for single fault detection in optical network," in *Proc. ICTON*, 2005.
- [21] C. Mas Machuca and M. Kiese, "Optimal placement of monitoring equipment in transparent optical networks," in *Proc. 6th Int. Workshop on Design and Reliable Communication Networks (DRCN)*, 2007.
- [22] A. Ferguson, B. O'Sullivan, and D. Kilper, "Transparent path length optimized optical monitor placement in transparent mesh networks," in *Optical Fiber Communication Conf. and Expo. and the Nat. Fiber Optic Engineers Conf.*, 2008, OThI3.
- [23] N. Sambo, Y. Pointurier, F. Cugini, L. Valcarenghi, P. Castoldi, and I. Tomkos, "Lightpath establishment assisted by offline QOT estimation in transparent optical networks," *J. Opt. Commun. Netw.*, vol. 2, no. 11, pp. 928–937, Nov. 2010.
- [24] J.-C. Antona, S. Bigo, and J.-P. Faure, "Nonlinear cumulated phase as a criterion to assess performance of terrestrial WDM systems," in *Optical Fiber Communications Conf.*, 2002, WX5.
- [25] F. Cugini, N. Sambo, N. Andriolli, A. Giorgetti, L. Valcarenghi, P. Castoldi, E. Le Rouzic, and J. Poirrier, "Enhancing GMPLS signaling protocol for encompassing quality of transmission (QoT) in all-optical networks," *J. Lightwave Technol.*, vol. 26, no. 19, pp. 3318–3328, Oct. 2010.
- [26] G. Agrawal, *Fiber-Optic Communication Systems*, 3rd ed. John Wiley & Sons Inc., 2002.
- [27] M. Angelou, Y. Pointurier, S. Azodolmolky, D. Careglio, S. Spadaro, and I. Tomkos, "A novel monitor placement algorithm for accurate performance monitoring in optical networks," in *Optical Fiber Communications Conf.*, 2011, JWA53.



Marianna Angelou (S'09) received a degree in computer science from the Aristotle University of Thessaloniki, Greece, in 2005. She received the M.Sc. in information and telecommunication technologies from Athens Information Technology in 2008 and is currently pursuing a Ph.D. with the Universitat Politècnica de Catalunya, Barcelona. In January 2008 she joined the "High-speed Networks and Optical Communications" Group of Athens

Information Technology, as a Research Scientist, working within the framework of EC-funded research projects. Her research activities focus on cross-layer optimization techniques for core optical networks and cover a broad range of topics in that area including physical layer awareness, energy-efficiency, and networking with flexible/adaptive transmission characteristics.



Yvan Pointurier (S'02–M'06) received a Diplôme d'Ingénieur from Ecole Centrale de Lille, France, in 2002, an M.S. in computer science in 2002, and a Ph.D. in electrical engineering in 2006, both from the University of Virginia, USA. He spent 2 years at McGill University in Montreal, Canada, as a Postdoctoral Fellow and then 1 year at Athens Information Technology, Greece, as a Technical Leader for a European Project. In 2009 he joined Alcatel-Lucent Bell Labs, France, as a Research Engineer. His research interests span design, optimization, and monitoring of networks in general and optical networks in particular. Dr. Pointurier is a co-recipient of the Best Paper Award at the IEEE ICC 2006 Symposium on Optical Systems and Networks.



Davide Careglio (S'05–M'06) received the M.Sc. and Ph.D. degrees in telecommunications engineering both from Universitat Politècnica de Catalunya (UPC), Barcelona, Spain, in 2000 and 2005, respectively, and the Laurea degree in electrical engineering from Politecnico di Torino, Turin, Italy, in 2001. He is currently an Associate Professor in the Department of Computer Architecture at UPC. Since 2000, he has been a Staff Member of the Advanced Broadband Communication Center (<http://www.ccaba.upc.edu>). His research interests include networking protocols with emphasis on optical switching technologies and algorithms and protocols for traffic engineering and QoS provisioning.



Salvatore Spadaro (M'10) received the M.Sc. (2000) and the Ph.D. (2005) degrees in telecommunications engineering from Universitat Politècnica de Catalunya (UPC). He also received the Dr. Ing. degree in electrical engineering from Politecnico di Torino (2000). He is currently an Associate Professor in the Optical Communications group of the Signal Theory and Communications Department of UPC. Since 2000 he has been a staff member of the Advanced Broadband Communications Center (CCABA) of UPC and he is currently participating in the STRONGEST FP7 EU project. In the past he was participating in the DICONET and BONE FP7 EU projects. He has co-authored about 90 papers in international journals and conferences. His research interests are in the fields of all-optical networks with emphasis on traffic engineering and resilience.



Ioannis Tomkos is the head of the "High-Speed Networks and Optical Communication (NOC)" Research Group at Athens Information Technology. NOC participates in many EU-funded research projects, in several of which Dr. Tomkos has a consortium-wide leading role (he is/was the Project Leader of the EU ICT STREP project ACCORDANCE, Project Leader of the EU ICT STREP project DICONET, Technical Manager of the EU IST STREP project TRIUMPH, Chairman of the EU COST 291 project, and WP leader and Steering Board member for several other projects). Dr. Tomkos has received the prestigious title of "Distinguished Lecturer" of IEEE Communications Society. Together with his colleagues and students he has authored about 380 articles/presentations (about 220 IEEE-sponsored archival items) and his work has received over 1500 citations.